EASR

Engineering and Applied Science Research

https://www.tci-thaijo.org/index.php/easr/index

Published by the Faculty of Engineering, Khon Kaen University, Thailand

Long-term rainfall forecasting using deep neural network coupling with input variables selection technique: A case study of Ping River Basin, Thailand

Uruya Weesakul*, Krisada Chaiyasarn and Shekhar Mahat

Department of Civil Engineering, Faculty of Engineering, Thammasat University 12120, Thailand

Received 7 July 2020
Revised 6 October 2020
Accepted 14 October 2020

Abstract

Long-term rainfall forecast is essential for water resources planning and management. Various approaches for forecasting have been developed, however, the accuracy of the forecast is still not satisfied for real engineering practice, particularly for monthly rainfall forecast with leading time of one-year ahead. This study aims to investigate the capability of the machine learning approach in the forecasting of monthly rainfall by using Deep Learning Neural Network (DNN) as a tool for calculation. Ping river basin, situated in the northern part of Thailand, was selected as a study area due to its availability of long time series of rainfall data. Six rainfall stations, distributed over the river basin, were selected for analysis using monthly rainfall from 1975 to 2018. The stochastic efficiency (SE) and correlation coefficient (r) were used for evaluation of model performance. Based on previous studies in this area, it has been revealed that 24 large-scale atmospheric variables (LAV), which were used as predictors in the DNN model, have correlations with seasonal rainfall over the Ping river basin. The result of the first simulation using all 24 LAV during the validation period (2009-2018) in predicting monthly rainfall for six rainfall stations for one-year ahead indicates that DNN is capable of forecasting with an accuracy of the forecast ranging from 58% to 72% with correlation coefficient from 0.59 to 0.82. Further improvement of the forecast was also conducted by the input selection technique resulting in a reduction of input LAV from 24 to 13 LAV. The second simulation of DNN with the input selection technique reveals that DNN provides better accuracy of the forecast for one-year ahead with the stochastic efficiency of the forecast ranging from 69% to 78%, with correlation coefficient from 0.75 to 0.82 for all stations.

Keywords: Rainfall forecasting, Deep learning neural network, Input selection technique, Thailand, Large-scale atmospheric variables

1. Introduction

Accurate rainfall forecasting is imperative in planning and management of water resources because it can convey valuable information to mitigate natural hazards. Forecasting rainfall is still a challenging task due to the complex atmospheric phenomenon so far. Many methods had been already attempted for forecasting rainfall in many parts of the world. In a reference from the literature study of hydrological time series forecasting of rainfall, artificial intelligence approaches namely artificial neural network (ANN), support vector regression (SVR), support vector machine (SVM), adaptive neuro-fuzzy inference system (ANFIS) and time-delay neural network were most prominent methods used in hydrology. The SVM and random forest were implemented to forecast real-time radar derived rainfall with 1-3 hours ahead in Taiwan. Overall, the SVM performed better than the random forest in all cases of the single-mode forecasting model [1]. Advantages of the ANFIS model over the other neural network models had been discussed in details for rainfall forecasting. It had been revealed that the ANFIS model outperformed in terms of performance [2, 3]. Another attempt to give insights of the ANN model over the multiple non-linear regression for the long-range forecast of Indian summer monsoon rainfall in India had been conducted. The results showed that the ANN model performed better than multiple non-linear regression model [4].

The ANN with back propagation method had been already implemented for monthly rainfall forecasting in India with 1 and 2-months lead period [5] and in Iran [6]. The ANN with mutual information technique was proposed to forecast rainfall in Mumbai, India. The model with mutual information performed better than the basic ANN model [7]. Global circulation model, ANN and ANFIS were used for prediction of rainfall and temperature changes in the long-term future over a Qassim, Saudi Arabia. The global circulation model showed better performance than other models [8]. The ANN with centripetal accelerated particle swarm optimization algorithm, gravitational search algorithm and imperialist competitive algorithm was proposed to forecast monthly rainfall in Malaysia. The result revealed that ANN consisting of centripetal accelerated particle swarm optimization algorithm showed better performance compared to the remaining algorithm with data preprocessing technique [9]. The ANN was proposed for forecasting Indian summer monsoon rainfall in India. The result revealed that the proposed ANN was able to predict the seasonal rainfall for the next 5 years in advance [10]. Similarly, the ANN was formulated to forecast hourly rainfall in Thailand with 1-3 hours in advance. Although ANN was tested for up to 6 hours lead period, the result of the simulation was acceptable for only up to 3 hours ahead [11].

Time-delay neural network and an autoregression integrated moving average model were implemented to forecast heavy monthly rainfall with a 1-month lead period for a flood-prone area in Malaysia. The finding revealed that time-delay neural

*Corresponding author.
Email address: wuruya@engr.tu.ac.th
doi: 10.14456/easr.2021.23

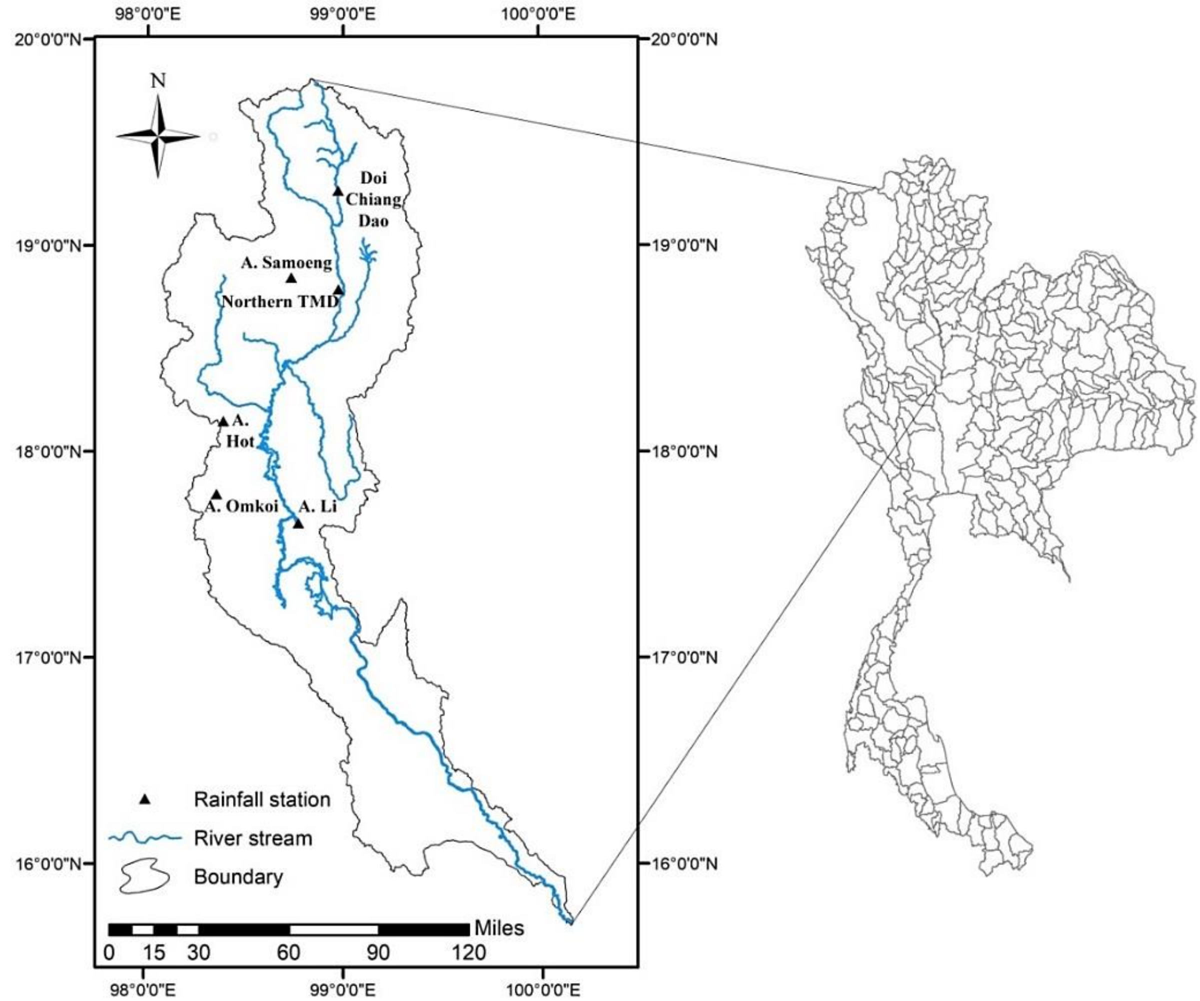

Figure 1 Ping river basin and rainfall stations location used in the study

network was capable of forecasting rainfall accurately than an autoregression integrated moving average [12]. The ANN, ANFIS and least square support vector machine were proposed to predict precipitation in Turkey. The study revealed that ANN performed better than the other models [13]. A recurrent neural network and long short-term memory were implemented to forecast monthly rainfall using long-sequential data in India. Both models had the ability to forecast the rainfall, however, long short-term memory outperformed the recurrent neural network in terms of accuracy [14]. The ANN with backpropagation, radial basis function and kriging method were proposed to predict monthly precipitation in China. The outcomes revealed that radial basis function performed better than the other models [15].

The ANN with feed-forward back propagation, cascade-forward back propagation neural network, distributed time-delay neural network and nonlinear autoregressive exogenous network were proposed for forecasting daily rainfall with a one-day advance in India. The findings of the study revealed that nonlinear autoregressive exogenous network outperformed the remaining models [16]. The SVM and ANN were implemented to predict monthly precipitation in Iran. The results revealed that SVM outperformed the ANN with higher capability of forecasting [17]. The ANN being composed of a wavelet analysis technique was proposed to forecast monthly rainfall in India. The study revealed that ANN with the wavelet analysis model performed better than simple artificial neural network and linear autoregressive model [18].

A hybrid support vector regression model, being composed of support vector regression and firefly algorithm, was implemented to forecast monthly rainfall with 1-month ahead in northwest Iran. The developed hybrid model outperformed basic support vector regression model [19]. A novel hybrid intelligent model, consisting of the ANFIS and firefly optimization algorithm, was proposed to forecast monthly rainfall with one-month lead time in Malaysia. Compared with performance criteria, the hybrid model outperformed the standard ANFIS for rainfall forecasting [20]. The SVM coupling with wavelet analysis was proposed to forecast monthly rainfall with 1, 3 and 6-month lead period in China. Evaluation of results showed that the proposed model was superior to that of simple ANN and SVM for the different lead period due to wavelet transform effect [21].

Recently, the capability of deep neural network (DNN) model was tested for forecasting monthly rainfall over a Khlong Yai river basin in the eastern region of Thailand. The result revealed that DNN was able to forecast monthly rainfall with acceptable accuracy for 3 months leading time of forecast [22].

In this study, it is aimed to investigate further development and performance of DNN model in the forecasting of monthly rainfall for one year ahead over the Ping river basin with sufficient availability of time series for analysis.

2. Data collection and study area

Based on the advantage of DNN in learning of behavior of historical data, river basin with long time series of rainfall data, Ping river basin, was selected as a case study. Ping river basin, covering a drainage area of about 35,000 square kilometers, is situated in the northern part of Thailand. Amongst 30 rainfall stations, distributed over the river basin, only 6 rainfall stations as presented in Figure 1, were selected in this study due to their reliability and consistency of data. Monthly rainfall data from

Table 1 Statistics of monthly and annual rainfall during training period (1975–2008) and validation period (2009-2018) of six rainfall stations used in the study

Stations	Location		Phase	Monthly Rainfall (mm)						Annual rainfall(mm)	
	Latitude	Longitude		Min.	Mean	Max.	S. D	Range	No. of data	Mean	S. D
A. Omkoi (327008)	17° 47' 24" N	98° 21' 36" N	Training	0	86	420	84	420	408	1034	201
			Validation	0	90	296	78	296	120	1081	174
A. Samoeng (327009)	18° 50' 24" N	98° 43' 48" E	Training	0	94	846	107	846	408	1136	365
			Validation	0	99	332	89	332	120	1188	152
Doi Bo Kaeo Seed Multiplication, A. Hot (327027)	18° 8' 60" N	98° 23' 24" E	Training	0	89	479	91	479	408	1075	213
			Validation	0	99	450	97	450	120	1184	216
Northern TMD (327501)	18° 47' 24" N	98° 58' 12" E	Training	0	98	455	96	455	408	1150	222
			Validation	0	95	471	96	471	120	1140	201
Ban Ko, A. Li (329006)	17° 38' 60" N	98° 46' 12" E	Training	0	82	339	80	339	408	985	164
			Validation	0	59	287	64	287	120	713	177
Doi Chiang Dao Watershed Research (327026)	19° 15' 36" N	98° 58' 12" E	Training	0	122	827	123	827	408	1469	358
			Validation	0	116	451	115	451	120	1394	242

Note. Min., Max., no., and S.D stand for minimum, maximum, number, and standard deviation, respectively.
Source: Thai Meteorological Department (2019)

these six rainfall stations during 1975-2018 were collected from the Thai Meteorological Department. Time series of monthly rainfall data was divided into two parts. The first part from 1975 to 2008 (around 77%) were used for analysis in training phase, while the second one beginning from 2009 to 2018 (around 23%) were used for the model validation process. Preliminary analysis of rainfall characteristics over the river basin is presented in Table 1.

3. Identification of large-scale atmospheric variables (LAV) influencing rainfall over ping river basin

Several kinds of research had been conducted to investigate the influence of large-scale atmospheric variables (LAV) on seasonal rainfall over different river basins in Thailand. The relationships between several LAV and seasonal rainfall over the Nan river basin, situated in the north of Thailand, was analyzed [23]. Followed by another study of relationships between a variety of LAV and seasonal rainfall over Chi and Mun river basins, which is located in the north-east of Thailand, was conducted [24, 25]. Relationships between various LAV and seasonal rainfall over the Tapee river basin, situated in the southern part of Thailand, was also investigated [26]. Such previous studies revealed that relationships between LAV and seasonal rainfall varied from basin to basin and season to season. However, the most common LAV, which influenced seasonal rainfall for all river basins, were Sea Level Pressure (SLP), Sea Air Temperature (SAT), Surface Zonal Wind (u), and Surface Meridian Wind (υ) [23-26]. Generally, the LAV time series can be retrieved from the Earth System Research Laboratory (ESRL). There are varieties of LAV, each LAV is composed of many atmospheric layers with different altitude from the earth. Each value of LAV represents mean value over a grid cell of 2.5^0 latitude × 2.5^0 longitude. The ERSL forecasts and provides monthly LAV time series, covering the area between longitude 60^0 E to 160^0 E and latitude 20^0 N to 20^0 S.

In this study, the selection of LAV, to be input to the DNN model, was based on the results of the analysis of the correlation between seasonal rainfall over the Ping river basin and LAV. Such analysis was conducted in another study. It was assumed in a study that when the correlation coefficient between seasonal rainfall and LAV was greater than 0.5, then such LAV was identified to be LAV influencing rainfall over the river basin [22]. Table 2 summarizes results from the analysis showing all LAV that are selected to be input to the DNN model in this study.

4. Formulation of Deep Neural Network (DNN) model for rainfall forecast

A soft computing technology such as artificial neural network, which inspired by the function and structure of the human brain, is a popular computational tool. The ANN constitutes of neurons, which are simple processing elements interconnected between the layers in the neural network. The information obtained in the form of input signals from other nodes or external stimuli in each node. Through an activation function, the information is processed locally and the transferred output signal is produced to other nodes or external outputs in the nodes. Then, the external information is fed in the input layer. Finally, the output is obtained in the output layer. Between the input and output layer, one or more intermediate layers are connected in the form of hidden layers. The layers are fully connected through the nodes that act as a processing unit [27]. The ANN has been implemented over the past three decades in hydrological time series data forecasting. As rainfall is nonlinear in nature, one of the major points of ANN popularity is due to its capacity to identify the relationship between input and output without considering physical characteristics. When the data set contains measurement errors with noise, the ANN can extract valuable information with satisfactorily result [28]. The major difference between the ANN and deep DNN is the number of hidden layers in the neural network architecture. The ANN contains a single hidden layer, whereas the DNN contains multiple hidden layers. The DNN consists of a stack of multiple perceptrons as shown in Figure 2. The hidden layers, consisting more than two layers, had the capability of solving the complex problems [29]. One of the tedious and complicated tasks is to fix the number of hidden neurons. There is no universal and identical rule for finding the optimal number of neurons in the hidden layers. Trial and error method are conducted to determine the optimal number of neurons [30-32]. For the implementation of the DNN model in the current study, different numbers of neurons in different hidden layers were simulated during the training phase resulting in different models with different

Table 2 Large-scale atmospheric variables used in the study

Variable abbreviation	Variable Name	Height Based on atmospheric pressure (milli bar)	Latitude		Longitude	
			From	To	From	To
AT1	Air temperature	200	-20° S	-30° S	210° E	220° E
AT2	Air temperature	Surface	-5° S	-15° S	210° E	220° E
AT3	Air temperature	1000	-20° S	-25° S	90° E	100° E
GH1	Geopotential Height	925	5° N	-5° S	230° E	250° E
GH2	Geopotential Height	925	-20° S	-25° S	150° E	165° E
GH3	Geopotential Height	850	-25° S	-35° S	75° E	85° E
MW1	Meridional Wind	200	0° S	-5° S	120° E	130° E
MW2	Meridional Wind	150	25° N	-30° S	80° E	85° E
MW3	Meridional Wind	10	25° N	20° N	120° E	130° E
O1	Omega	400	0° E	-5° S	115° E	125° E
P1	Pressure	Surface	20° N	25° N	130° E	140° E
P2	Pressure	Surface	-15° S	-25° S	160° E	170° E
P3	Pressure	Surface	-25° S	-35° S	75° E	85° E
PW1	Precipitable Water	850	0° E	-10° S	115° E	125° E
RH1	Relative Humidity	850	-5° S	-10° S	110° E	25° E
RH2	Relative Humidity	850	-15° S	-25° S	125° E	130° E
SLP1	Sea level pressure	Surface	15° N	20° N	130° E	140° E
SLP2	Sea level pressure	Surface	-15° S	-25° S	160° E	170° E
SLP3	Sea level pressure	Surface	-25° S	-35° S	75° E	85° E
SST1	Sea surface temperature	Surface	5° N	10° N	120° E	130° E
SST2	Sea surface temperature	Surface	-15° S	-20° S	55° E	66° E
ZW1	Zonal wind	150	0° E	10° S	130° E	145° E
ZW2	Zonal wind	925	-10° S	-15° S	160° E	170° E
ZW3	Zonal wind	850	-25° S	-30° S	95° E	100° E

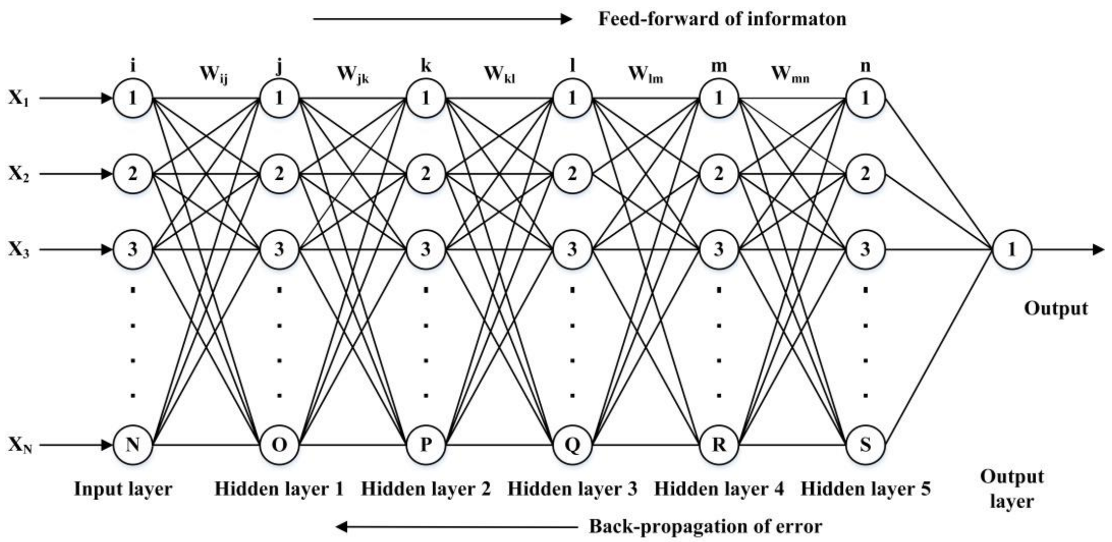

Figure 2 Deep learning neural network architecture [22]

numbers of neurons in five hidden layers. The time series data was divided in to two parts. Data from 1975 to 2008 for training phase (around 77%), while validation phase starting from 2009 to 2018 (around 23%). Google TensorFlow was used for deep neural network framework. The configuration of deep neural network has been performed with Language: Python 3.6, CPU: Intel core i7-7700 @ 3.60 GHz, RAM: DDR4 @ 16 GB, GPU: NVIDIA GeForce GT 730, and Library: Google TensorFlow 1.14.0.

4.1 Feed-Forward propagation

Input layer is feed from external data and output layer feeds data to external destination. At first, multiplication of each input node with random weight takes place. In the input layer, the input is received in each node with some random multiple weight. Through the activation function in each node, the summation of input and weight with bias takes place with the output. Likewise, for the other nodes in remaining layers, the same procedure occurs until in the output layer. The output is obtained in the hidden node as represented in the Eq. 1. The activation function, sigmoid function, is applied in each node as presented in Eq. 2. Error in the output node is obtained as shown in Eq. 3.

$$h_j = \sigma\left(z_j\right) = \sigma\left(\sum_{i=1}^{N} w_{ij} x_{ij} + b_j\right) \tag{1}$$

$$\sigma = \frac{1}{1+e^{-z_j}} \tag{2}$$

$$E = \frac{1}{2}\left(O-P\right)^2 \tag{3}$$

where σ is an sigmoid activation function, z_j is network input node of sigmoid activation function on hidden node j, b_j represents bias on hidden node j, x_{ij} indicates input of i value on hidden node j, w_{ij} denotes weight of i value on hidden node j, h_j represents output on hidden node j, O is observed output, and P is target output.

4.2 Backward propagation

The back-propagation algorithm dated back to 1960s but it gained popularity in 1986 [33]. In the back-propagation, the weights of the connections are adjusted to minimize the error between observed and target output. The back-propagation technique follows the gradient of network error to adjust weight in backward from output to input using the chain rule of differential calculus. The mathematical representation of backward propagation is shown in the following equations. Equation 4 shows the change of weight whereas Eq. 5 represents the updated weight in a network.

$$\delta_{w_{ij}} = \frac{\partial E}{\partial w_{ij}} = (\text{O-P})h_j' = (\text{O-P})Z_j(1\text{-}Z_j)Z_j' \tag{4}$$

$$w_{new_{ij}} = w_{old_{ij}} + \delta w_{ij} \tag{5}$$

Where $\delta_{w_{ij}}$ represents change of weight i value at hidden node j, h_j' is a derivative of activation function at hidden node j, z_j' is called derivative of network at node j, $w_{new_{ij}}$ presents new weight of i value at hidden node j, and $w_{old_{ij}}$ is old weight of i value at hidden node j.

In this study, the DNN model was implemented for each rainfall station using monthly rainfall data from 1975 to 2008 for the training process of the model. All 24 LAV, preliminary screened as mentioned in the previous section (Table 2), were used as input to the DNN model for all rainfall stations.

Once the DNN model was already trained for all rainfall stations from 1975 to 2008, the DNN model was used to forecast monthly rainfall for each station from 2009 to 2018 varying the leading time of forecast for 1, 3, 6 and 12-months to evaluate the performance of the model.

5. Model evaluation criteria

There are several model evaluation techniques to explore performance of model such as root mean square error (RMSE) [3], mean absolute error (MAE) [6], Nash-sutcliffe efficiency (NSE) [7], performance parameter (PP) [10], efficiency index (EI) [11], mean absolute percentage error (MAPE) [2], and correlation coefficient (r) [10] between measured data and computed value from model. Selection of model evaluation method depends on objective of study since each method has its own manipulation to explore errors or accuracy of forecast for specific purpose.

In this study two methods of model evaluation were selected. Firstly, stochastic efficiency (SE) of forecast was adopted to investigate how many times the forecasted rainfall falling within the observed value plus and minus standard deviation for the whole experimental events [22]. Secondly, correlation coefficient (r) was used to explore how well the forecasted rainfall associate with the observed rainfall [10].

5.1 Stochastic efficiency (SE)

Stochastic efficiency (SE) is an index that describes the accuracy of forecasted monthly rainfall within the standard deviation of observed rainfall for the particular month in terms of percentage. Higher the percentage of the forecast, the higher will be the accuracy of the model and vice versa. The zero percentage shows the poor capability of a forecasting model, while 100% denotes the maximum accuracy of the forecast. To calculate the stochastic efficiency, the following condition needs to be satisfied as presented in Eq. 6. Similarly, the stochastic efficiency is obtained as per Eq. 7.

$$\text{ROM}_{i,j} - \sigma_i \le \text{RPM}_{i,j} \le \text{ROM}_{i,j} + \sigma_i \tag{6}$$

$$\text{Stochastic efficiency (SE)} = \frac{P}{N} * 100\% \tag{7}$$

Where $\text{RPM}_{i,j}$ is forecasted monthly rainfall i (i = 1….12) in year j (j = 2009-2018), $\text{ROM}_{i,j}$ is observed monthly rainfall i (i = 1….12) in year j (j = 2009-2018), σ_i is standard deviation of monthly rainfall in month i (i = 1…12) during the years 2009-2018, P is a number of forecasted monthly rainfalls being in between mean observed monthly rainfall plus and minus standard deviation of monthly rainfall and N is the total number of rainfall observations for the validation period 2009-2018 i.e. 12 * 10 = 120 in this case.

5.2 Correlation coefficient (r)

Correlation coefficient is often used in numerous researches for model evaluation in hydrology applications to investigate the strength of relationship between two variables, which are the computed output by the model and the observed data. Its value ranges from -1 to +1. Perfect positive relationship is indicated by +1, while perfect negative relationship is indicated by -1 and zero means there is no relationship. In this study, linear relationship between the forecasted monthly rainfall and the observed monthly rainfall was aimed to be measured. Therefore, the correlation coefficient was selected, which can be calculated by the following formula shown in Eq. 8.

$$\text{Correlation coefficient (r)} = \frac{N\sum_{i=1}^{N} P_i O_i - \sum_{i=1}^{N} P_i \sum_{i=1}^{N} O_i}{\sqrt{\left[N\sum_{i=1}^{N} P_i^2 - \left(\sum_{i=1}^{N} P_i\right)^2\right]\left[N\sum_{i=1}^{N} O_i^2 - \left(\sum_{i=1}^{N} O_i\right)^2\right]}} \tag{8}$$

Where P_i is predicted rainfall of month i (i = 1….12) in the year 2009 to 2018, O_i is observed rainfall of month i (i = 1….12) in the year 2009 to 2018, N is total number of forecasted monthly rainfalls during 2009 to 2018, i.e., 12 * 10 = 120.

6. Performance of basic DNN model

Table 3 presents the performance of the DNN model in forecasting monthly rainfall over the Ping river basin during the period of validation (2009-2018). Simulations of the DNN model were conducted for all six rainfall stations, varying the leading time of forecast from 1, 3, 6 to 12 months. Figure 3 presents the plot of stochastic efficiency values for all stations for all leading time of forecast. It clearly shows that the performance of forecast in terms of stochastic efficiency decreases when the leading time of forecast increases for all cases (see Figure 3). The best performance of forecast is obtained at a one-month leading time of forecast at. A. Samoeng station with value of stochastic efficiency equal to 79.2% and correlation coefficient equal to 0.80. For long term forecast, i.e., one-year ahead, the best performance was also found at A. Samoeng station with value of stochastic efficiency equal to 71.7% and correlation coefficient equal to 0.82 (see Table 3). The lowest performance of model was found at A. Omkoi station with value of stochastic efficiency for one-month lead period equal to 68.3% and correlation coefficient equal to 0.72, and for 12-months leading time with

Table 3 Performance of deep neural network in forecasting of monthly rainfall up to one year ahead over Ping river basin during validation period (2009-2018)

Stations	Lead period							
	1-month		3-months		6-months		12-months	
	S. E	r	S. E	r	S. E	r	S. E	r
A. Samoeng	79.2	0.80	73.3	0.81	72.5	0.78	71.7	0.82
A. Omkoi	68.3	0.72	65.8	0.67	60.8	0.66	58.3	0.59
Doi Bo Kaeo Seed Multiplication, A. Hot	70.0	0.68	68.3	0.65	67.5	0.68	63.3	0.68
Northern TMD	75.8	0.72	73.3	0.69	70.0	0.69	69.2	0.67
Ban Ko, A. Li	74.2	0.67	71.7	0.74	67.5	0.73	65.0	0.74
Doi Chiang Dao Watershed Research	69.2	0.80	67.5	0.81	65.0	0.79	63.3	0.79

value of stochastic efficiency equal to 58.3% and correlation coefficient equal to 0.59. The second highest performance of model was found at Northern TMD station, followed by Ban Ko A. Li station, then Doi Bo Kaeo Seed Multiplication A. Hot station and Doi Chiang Dao Watershed Research station with stochastic efficiency values equal to 69.2%, 65.0%, 63.3% and 63.3% respectively for one-year ahead forecast (see Table 3).

An attempt to explain the behavior of DNN model by using characteristics of rainfall was conducted. Based on characteristic of monthly rainfall, presented in terms of statistical parameters during training and validation period of all six rainfall stations as shown in Table 1, it has been remarked that A. Samoeng station, whose stochastic efficiency is highest, has higher standard deviation of monthly rainfall (S.D=107) than A. Omkoi station, whose stochastic efficiency is lower (S.D=84). It has been also noted that A. Samoeng station, whose stochastic efficiency is highest, has higher range of monthly rainfall (0-846 mm) than A. Omkoi station with a lower range of monthly rainfall (0-420 mm). However, for others four rainfall stations, Northern TMD, Ban Ko A. Li, Doi Bo Kaeo Seed Multiplication A. Hot and Doi Chiang Dao Watershed Research station, their values of S.D are not ranked systematically which are 96, 80, 89 and 123 respectively. The range of monthly rainfall stations of these rainfall stations varies from station to station which are (0-455 mm), (0-339 mm), (0-479 mm) and (0-827 mm) for Northern TMD, Ban Ko A. Li, Doi Bo Kaeo Seed Multiplication A. Hot and Doi Chiang Dao Watershed Research stations respectively. The basic statistical properties of monthly rainfall are not corresponding to ranking of performance of model; therefore, it cannot be used to explain behavior of model performance represented by stochastic efficiency in this particular case.

Nevertheless, based on the values of stochastic efficiency, ranging from zero to 100%, all of the stations provide stochastic efficiency more than 50% for all cases. It implies that forecasted monthly rainfall are acceptable correct (forecasted value falling in between observed value plus and minus standard deviation) with more than 50% of correct forecasted events.

7. Improvement of accuracy of forecast using input selection approach

Input variables selection methods are categorized in three types i.e. wrapper, embedded and filter approach. In any data-driven statistical model, the selection of optimal input variables is fundamental and crucial steps. Machine learning model, such as the ANN model, is often developed without considering the effect of input variables on model performance [34]. Selecting the appropriate relevant and elimination of irrelevant feature are central issues in machine learning [35]. Through the input selection approach, only relevant input variables are taken into consideration [34, 35]. The neural network-based model performs more accurately once the optimal set of input variables is identified [34]. More comprehensive literature context on input variables selection techniques can be further studied for details [34-36]. Input variables selection approach using the neural network was already implemented in hydrology for streamflow forecasting [37] and rainfall forecasting [38]. Data driven models using input selection methods improved the performance significantly [37, 38]. To select the optimal input variables before formulating the final DNN model for rainfall forecasting, the input selection technique, filter approach, was used in this study because filter approach excludes irrelevant attributes and independent to algorithm. Moreover, it evaluates every individual feature on the basis of high correlation with the output [34, 35].

The effort of improvement of accuracy of the forecast was conducted in this study. More predictive variables, to be an input of the DNN model, were selected by ranking performance of forecast of each individual variable one by one for each station. Performance of forecast was measured by stochastic efficiency and correlation coefficient. As described earlier in performance evaluation criteria section, values of stochastic efficiency ranges from 0% to 100%, therefore, it was considered that variable having stochastic efficiency (SE) of forecast greater than 50% was more predictive variable than variables having stochastic efficiency less than 50%. Therefore, such assumption was used as the criteria for selecting the variables having SE values greater than 50% to be input to the DNN model [22]. In this particular case, it was assumed that LAV with SE value from 55% and higher was good enough to influence monthly rainfall, as an output of the DNN model.

Table 4 presents the ranking of the stochastic efficiency of each input as the input to the DNN model in forecasting monthly rainfall for one month ahead during the validation period (2009-2018). Based on selection criteria of input, with SE greater than 55%, 14 LAV were selected as input to DNN model, which are Air temperature (AT2, AT3), Sea Surface Temperature (SST1, SST2), Zonal wind (ZW1, ZW2, ZW3), Meridian Wind (MW1, MW2), Relative Humidity (RH1, RH2), Precipitable Water (PW1), Geopotential Height (GH2) and Omega (O1). It was also remarked that monthly rainfall at the station itself (IRF) with a lagging time of one month was also included in this performance analysis. The results of the analysis, as presented in Table 4, showed that there existed a relationship between previous rainfall and present rainfall for all of the rainfall stations, therefore, monthly rainfall at its own station with different lagging time, depending on leading time of the forecast, were included as input to DNN model. Analysis of the best combination of selected LAV input to the DNN model was conducted at each rainfall station.

For each combination of selected LAV as well as previous monthly rainfall, simulation of the DNN model, during the validation period (2009-2018), was conducted in order to determine the best architecture of DNN, providing the best performance of forecast. Table 5 illustrated the best architecture of the DNN model for each combination of LAV input.

A comparison of the performance of different DNN models, as shown in Table 5, at each station was done by using stochastic efficiency (SE) of the forecast and correlation coefficient (r) as criteria. Table 6 summarized the performance of different DNN models in forecasting monthly rainfall with a one-month leading time of forecast for all stations. It has been revealed that best performance exhibited by Model 13 at A. Samoeng station with value of stochastic efficiency equal to 85% and correlation

Table 4 Performance of each LAV in forecasting of monthly rainfall for one month ahead over Ping river basin during validation period (2009-2018)

Rank	A. Samoeng			A. Omkoi			Doi Chiang Dao Watershed Research			Doi Bo Kaeo Seed Multiplication, A. Hot			Northern TMD			Ban Ko, A. Li		
	LAV	SE	r	LAV	SE	r	LAV	SE	r	LAV	SE	r	LAV	SE	r	LAV	SE	r
1	AT3	84.2	0.82	MW2	72.5	0.66	IRF	71.7	0.77	IRF	75.0	0.69	SST2	76.7	0.74	IRF	75.8	0.75
2	ZW2	83.3	0.80	SST2	71.7	0.70	ZW2	70.8	0.84	MW2	75.0	0.71	MW1	75.8	0.77	ZW2	74.2	0.75
3	MW1	78.3	0.79	ZW2	71.7	0.71	AT3	68.3	0.78	ZW2	74.2	0.76	AT3	74.2	0.75	MW1	70.8	0.67
4	MW2	78.3	0.75	AT3	70.8	0.72	MW1	67.5	0.77	MW1	71.7	0.71	MW2	74.2	0.71	AT3	70.0	0.73
5	IRF	77.5	0.72	GH2	70.8	0.68	MW2	67.5	0.73	SST2	69.2	0.70	ZW2	73.3	0.74	MW2	70.0	0.67
6	SST2	75.8	0.80	MW1	70.0	0.64	SST2	66.7	0.80	AT3	67.5	0.65	IRF	71.7	0.68	SST2	66.7	0.76
7	RH2	74.2	0.75	RH2	67.5	0.67	RH2	62.5	0.75	GH2	67.5	0.59	PW1	70.8	0.70	AT2	65.8	0.60
8	PW1	72.5	0.77	IRF	65.8	0.68	SST1	62.5	0.71	RH2	67.5	0.62	GH2	69.2	0.69	GH2	64.2	0.62
9	RH1	72.5	0.73	SST1	65.0	0.61	GH2	60.8	0.64	PW1	65.8	0.66	RH1	65.8	0.70	RH2	63.3	0.67
10	SST1	72.5	0.75	PW1	61.7	0.69	RH1	59.2	0.74	RH1	65.8	0.64	SST1	65.8	0.65	ZW3	61.7	0.43
11	AT2	70.8	0.74	RH1	58.3	0.66	PW1	57.5	0.75	AT2	62.5	0.63	ZW3	65.8	0.63	RH1	60.8	0.64
12	GH2	70.8	0.74	AT2	57.5	0.57	ZW1	56.7	0.55	SST1	60.0	0.62	RH2	64.2	0.70	SST1	60.0	0.58
13	ZW3	62.5	0.49	ZW1	56.7	0.42	AT2	55.8	0.65	ZW3	56.7	0.51	AT2	57.5	0.62	PW1	55.8	0.63
14	ZW1	57.5	0.46															
15	O1	55.8	0.52															

Table 5 Architecture of DNN model with different combination of LAV input

Model	Input combination	No. of variables	Architecture of DNN (number of neurons in each hidden layer)
1	AT3	1	[12, 4, 4, 4, 4, 4, 1]
2	AT3, ZW2	2	[24, 8, 8, 8, 8, 8, 1]
3	AT3, ZW2, MW1	3	[36, 12, 12, 12, 12, 12, 1]
4	AT3, ZW2, MW1, MW2	4	[48, 16, 16, 16, 16, 16, 1]
5	AT3, ZW2, MW1, MW2, IRF	5	[60, 20, 20, 20, 20, 20, 1]
6	AT3, ZW2, MW1, MW2, IRF, SST2	6	[72, 24, 24, 24, 24, 24, 1]
7	AT3, ZW2, MW1, MW2, IRF, SST2, RH2	7	[84, 28, 28, 28, 28, 28, 1]
8	AT3, ZW2, MW1, MW2, IRF, SST2, RH2, PW1	8	[96, 32, 32, 32, 32, 32, 1]
9	AT3, ZW2, MW1, MW2, IRF, SST2, RH2, PW1, RH1	9	[108, 36, 36, 36, 36, 62, 1]
10	AT3, ZW2, MW1, MW2, IRF, SST2, RH2, PW1, RH1, SST1	10	[120, 40, 40, 40, 40, 40, 1]
11	AT3, ZW2, MW1, MW2, IRF, SST2, RH2, PW1, RH1, SST1, AT2	11	[132, 44, 44, 44, 44, 44, 1]
12	AT3, ZW2, MW1, MW2, IRF, SST2, RH2, PW1, RH1, SST1, AT2, GH2	12	[144, 48, 48, 48, 48, 48, 1]
13	AT3, ZW2, MW1, MW2, IRF, SST2, RH2, PW1, RH1, SST1, AT2, GH2, ZW3	13	[156, 52, 52, 52, 52, 52, 1]
14	AT3, ZW2, MW1, MW2, IRF, SST2, RH2, PW1, RH1, SST1, AT2, GH2, ZW3, ZW1	14	[168, 56, 56, 56, 56, 56, 1]
15	AT3, ZW2, MW1, MW2, IRF, SST2, RH2, PW1, RH1, SST1, AT2, GH2, ZW3, ZW1, O1	15	[180, 60, 60, 60, 60, 60, 1]

Remark: IRF is monthly rainfall station at corresponding station with lagging time

coefficient equal to 0.83, while the lowest performance recorded by Model 11 at Doi Chiang Dao Watershed research station with value of stochastic efficiency equal to 74.2% and correlation coefficient equal to 0.81 (see Table 6). It was also revealed that the best DNN model varied from station to station with a different combination of LAV.

The best DNN model, with a different combination of LAV, at each station was then used to forecast monthly rainfall with a different leading time of the forecast, i.e., 1, 3, 6 and 12-months. Stochastic efficiency of forecast at each station for all cases was manipulated and compared with the result obtained previously from the DNN model without the input section technique as presented in Figure 3.

It has been revealed that the input selection technique can improve the accuracy of the forecast in all rainfall stations (see Figure 3). Based on the value of stochastic efficiency as performance of forecast criteria (see Table 3 and Table 7), DNN model with input selection technique performs better than DNN model without input selection technique with higher value of stochastic efficiency for all leading time of forecast. For each rainfall stations, performance of forecast of DNN model technique decreases when leading time of forecast increase as shown in Figure 3.

For one-year leading time of forecast, where performance of forecast is lowest for all stations, similar results were obtained. Performance of forecast for one-year ahead was highest at A. Samoeng station with value of stochastic efficiency equal to 77.5% and correlation coefficient equal to 0.82. The lowest was obtained at Doi Chiang Dao Watershed Research and Doi Bo Kaeo Seed Multiplication A. Hot station with value of stochastic efficiency equal to 69.2% (see Table 7).

Based on the value of stochastic efficiency as model performance index, varying from zero to 100 percent of accuracy of forecast, stochastic efficiency greater than 50% means more than 50% of event are acceptable with the forecasted value falling in between observed value plus and minus standard deviation. Therefore, criteria used in this study is that when value of stochastic efficiency of model greater than 50%, the performance of model is acceptable.

For all rainfall stations, performance of model of all leading time is acceptable (see Figure 3 and Table 7) with values of stochastic efficiency greater than 50%. However, performance of model in forecasting varies from station to station. The highest

Table 6 Stochastic efficiency of monthly rainfall forecast for 1-month leading time of forecast provided by different DNN models

	Model	1	2	3	4	5	6	7	8	9	10	11	12	13	14	15
A. Samoeng	SE	83.3	85.0	80.0	80.0	74.2	76.7	80.8	80.0	80.0	80.8	77.5	80.8	**85.0**	83.3	83.3
	r	0.83	0.81	0.81	0.74	0.77	0.78	0.77	0.76	0.78	0.79	0.79	0.81	**0.83**	0.81	0.82
A. Omkoi	SE	70.0	71.7	74.2	75.0	**75.0**	74.2	73.3	73.3	74.2	73.3	70.8	74.2	73.3		
	r	0.65	0.67	0.68	0.69	**0.73**	0.72	0.73	0.71	0.68	0.71	0.68	0.71	0.69		
Doi Bo Kaeo Seed Multiplication, A. Hot	SE	72.5	67.5	65.8	68.3	69.2	65.0	71.7	71.7	71.7	72.5	73.3	72.5	**75.0**		
	r	0.62	0.58	0.62	0.66	0.66	0.67	0.73	0.74	0.73	0.74	0.75	0.74	**0.72**		
Northern TMD	SE	76.7	79.2	79.2	72.5	**80.0**	72.5	77.5	79.1	78.3	76.7	80.0	77.5	75.8		
	r	0.75	0.76	0.75	0.74	**0.76**	0.7	0.74	0.75	0.75	0.73	0.75	0.74	0.74		
Ban Ko, A. Li	SE	74.2	75	71.7	69.2	69.2	69.2	69.2	79.2	78.3	77.5	**79.2**	76.7	76.7		
	r	0.73	0.76	0.72	0.66	0.71	0.60	0.72	0.75	0.74	0.78	**0.77**	0.74	0.78		
Doi Chiang Dao Watershed Research	SE	68.3	70.0	67.2	74.2	70.0	72.5	72.5	74.2	73.3	74.2	**74.2**	71.7	70.8		
	r	0.78	0.77	0.74	0.76	0.75	0.76	0.75	0.78	0.78	0.80	**0.81**	0.79	0.8		

Table 7 Stochastic efficiency of monthly rainfall for 1 month, 3 months, 6 months, and one-year leading time of forecast during validation period (2009-2018)

Stations	Model	Lead period							
		1-month		3-months		6-months		12-months	
		S. E	r	S. E	r	S. E	r	S. E	r
A. Samoeng	13	85	0.83	84.2	0.81	82.5	0.83	77.5	0.82
A. Omkoi	5	75	0.73	73.3	0.72	72.5	0.69	71.7	0.70
Doi Bo Kaeo Seed Multiplication, A. Hot	13	75	0.72	72.5	0.76	70.0	0.75	69.2	0.77
Northern TMD	5	80	0.76	76.7	0.73	73.3	0.73	72.5	0.76
Ban Ko, A. Li	11	79.2	0.77	78.3	0.8	75.8	0.76	72.5	0.75
Doi Chiang Dao Watershed Research	11	74.2	0.81	71.7	0.81	70.0	0.81	69.2	0.81

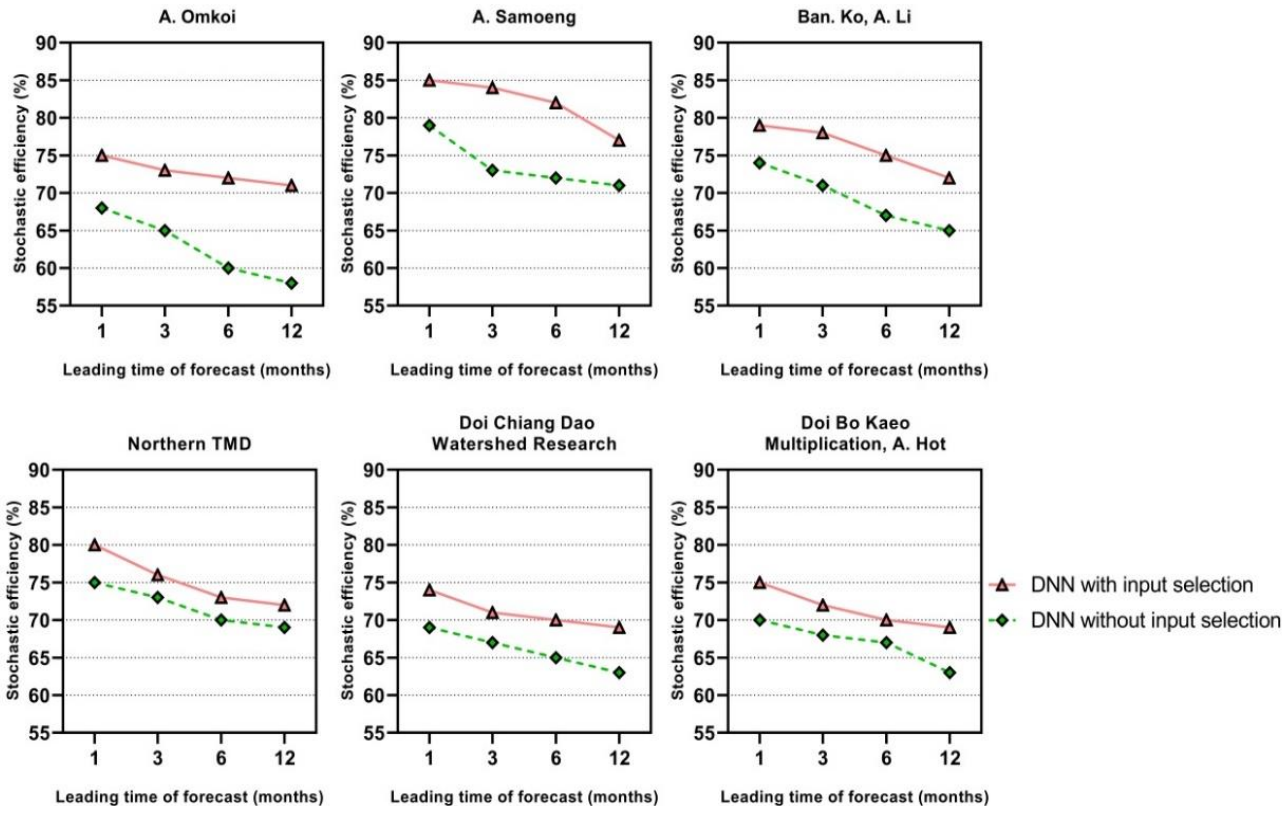

Figure 3 Performance of DNN model with and without input selection technique for different leading time of forecast

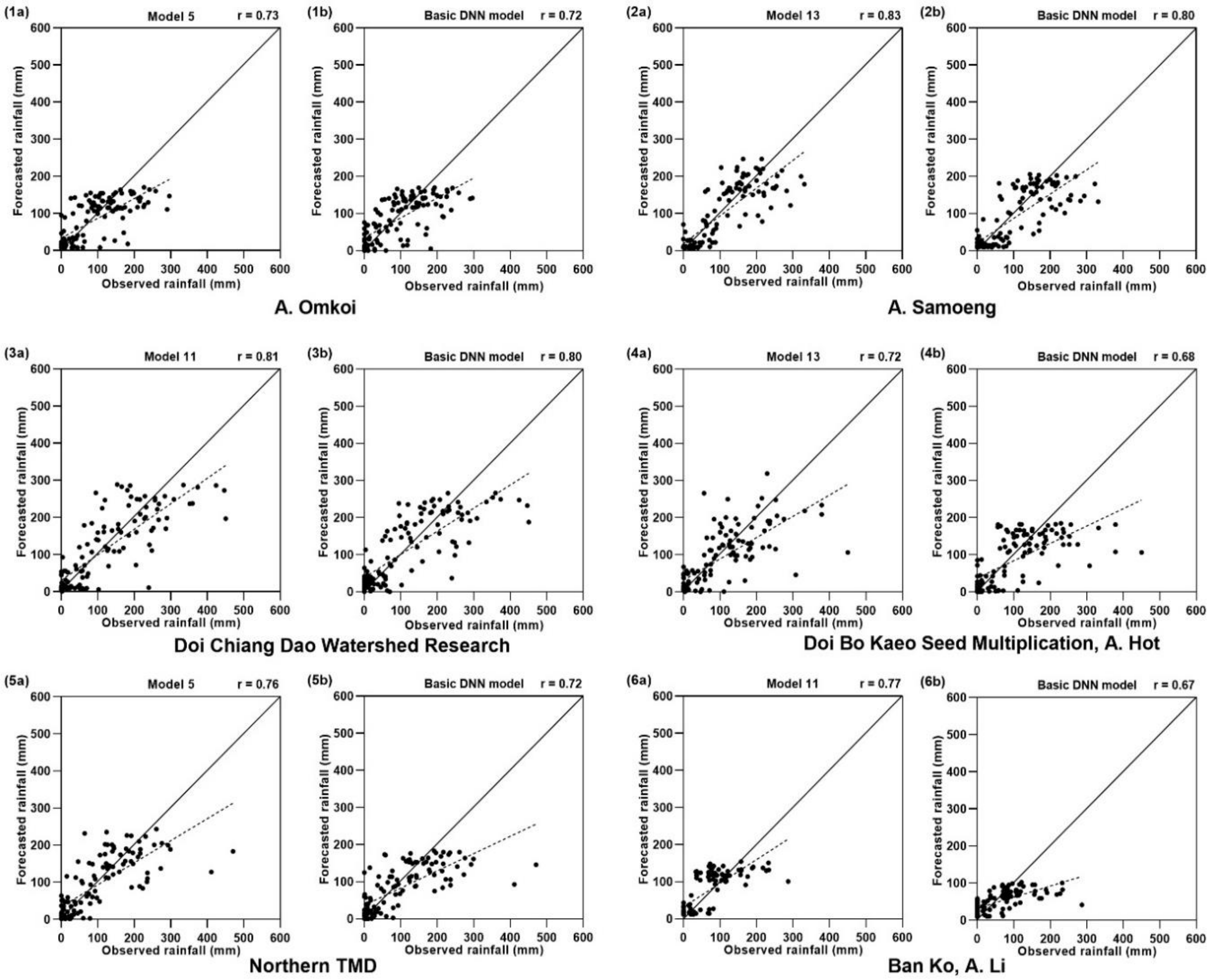

Figure 4 Correlation coefficient comparison of observed and forecasted rainfall for 1-month lead period for validation period 2009-2018

performance is at A. Samoeng station (with stochastic efficiency equal to 85% for one-month lead period and stochastic efficiency equal to 77.5% for 12-months leading time) as shown in Figure 3. The second-best performance recorded at Ban Ko A. Li and Northern TMD, then A. Omkoi, followed by Doi Bo Kaeo Seed Multiplication A. Hot and Doi Chiang Dao Watershed Research station for 12-months leading time in the descending order of stochastic efficiency. The lowest performance of forecast was found at Doi Chiang Dao Watershed Research station with value of stochastic efficiency equal to 74.2% for one-month leading time and stochastic efficiency equal to 69.2% for 12-months leading time.

It has been revealed that association between observed and forecasted monthly rainfall was improved when DNN model coupling with input selection technique for all stations (see Figure 3, Table 3, Table 7) for all lead periods of forecast. For example, Table 3 and Table 7 revealed that correlation coefficients between observed and forecasted monthly rainfall for 12-months lead period of basic DNN models have values from 0.59 to 0.82, which increased between 0.70 to 0.82 when DNN model coupling with input selection technique was used for simulation.

Figure 4 presents scatter plots as well as correlation coefficient between observed and forecasted monthly rainfall for one-month lead period. It reveals that DNN model coupling with input selection technique provides better association between observed and monthly rainfall for all stations with increasing in values of correlation coefficients. Figure 5 presents example plots of time series of observed and forecasted monthly rainfall for one-month lead period for three stations. It has been noticed that low performance occurred with extremely high rainfall.

8. Discussion

Based on model evaluation parameters in this study, which are stochastic efficiency and correlation coefficient, the results show that the proposed input selection technique with Deep Neural Network can improve model performance in all stations for all different leading time of forecast. This is because only more predictive variables are selected to be input to the model. However, the optimum number of input variables to the DNN model cannot be observed systematically in this study for all stations. Table 5, presenting how the number of input variables affect the accuracy of forecast, reveals that there is no association between number of input variables with stochastic efficiency, nor correlation coefficient at each station. The optimum number of input variables varies from station to station, resulting in different DNN model for different stations (see Table 5). However, there exist the same optimal number of input variables at A. Omkoi and Northern TMD stations with five input variables, Ban Ko A. Li, Doi Chiang Dao Watershed Research stations with 11 input variables, and A. Samoeng and Doi Bo Kaeo Seed Multiplication A. Hot stations with 13 inputs variables.

Considering rainfall characteristics in the study area, presented by basic statistical properties of monthly and annual rainfall at each stations in Table 1, it shows that mean monthly

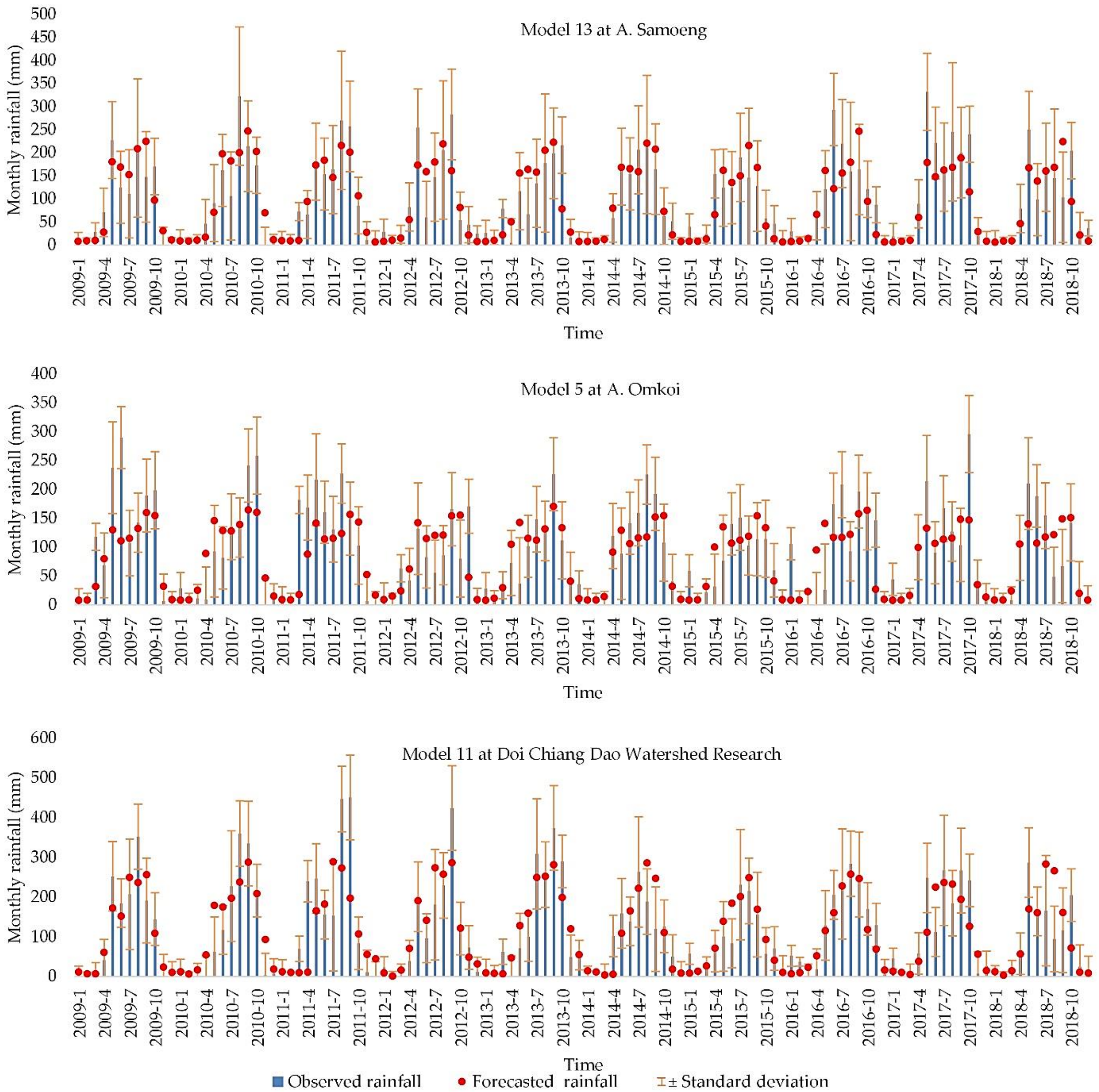

Figure 5 Comparison between observed and forecasted rainfall for 1-month lead period during validation period 2009-2018

rainfall are not much different for both in training period and validation period varying from 86 mm to 122 mm except for Ban Ko A. Li where mean monthly rainfall is lowest with value of 59 mm in validation period and 82 mm in training period. However, for extreme values of monthly rainfall, there exists high differences at A. Samoeng station with maximum monthly rainfall equal to 846 mm and Doi Chiang Dao Watershed Research station with maximum monthly rainfall equal to 827 mm. The other stations have similar maximum monthly rainfall of value ranging from420 mm to 479 mm (except at Ban Ko A. Li station where maximum monthly rainfall equal to 339 mm). This implies high variation in extreme value in the study area.

Nevertheless, standard deviations of monthly rainfall are not much different for all stations. For interannual variation of rainfall at each station, there is variation, represented by standard deviation of annual rainfall, from 201 mm to 365 mm. The difference of model performance at each station cannot be described by these basic statistical properties of rainfall in this case study.

Typically, the DNN model, as Artificial Intelligence (AI) approach model, is dependent on the range (minimum and maximum) of the training data set, and in case that the validation data set differs in the range of training data, the performance of model decreases. In this study, the problem of out-of-range does not occur due to the sufficient long time series in training data covering the extreme value in validation period as shown in Table 1, where maximum monthly rainfall in validation period is lower than that of training period of all stations.

However, Figure 5, showing comparison between observed and forecasted monthly rainfall for one-month leading time of forecast for three rainfall stations as examples, reveals that DNN model always underestimate the extreme values for all stations. Similar remark was found in Figure 4, showing scattered plot between observed and forecasted monthly rainfall for one-month leading time for all stations. It has been observed from Figure 5 that forecasted monthly rainfall are often underestimated where its value exceeds its mean plus standard deviation. The model tries to minimize overall error of forecast by forecasting not far from mean plus standard deviation. The model, proposed in this study, is not appropriate for flood forecasting. However, comparison of scatter plots between results obtained in case of basic DNN model and DNN model with input selection technique for all station, presented in Figure 4, reveals that the proposed technique can improve the estimation of extreme rainfall with the values closer to observed one than case of basic DNN model.

9. Conclusions

Investigating the capability of the machine learning approach in the forecasting of monthly rainfall for the long-term by using Deep Learning Neural Network as a computational tool was conducted in the study. Ping river basin, situated in the northern part of Thailand, with the availability of reliable and consistent monthly rainfall time series for 6 rainfall stations, was selected as a case study. Influential 24 large-scale atmospheric variables, retrieved from their high correlation with seasonal rainfall over the river basin, were used as input to the DNN model. Acceptable accuracy of long-term forecast for one-year ahead was obtained with the value of stochastic efficiency of forecast varied from 58% at A. Omkoi station with correlation coefficient equal to 0.59 to 72% at A. Samoeng station with correlation coefficient equal to 0.82. Further improvement of accuracy of the forecast was performed by using the input selection technique to screen only the most predictive large-scale atmospheric variables to be input to the DNN model. Results of simulation of DNN model coupling with the input selection technique showed that improvement of accuracy of the forecast was achieved for one-year leading time of forecast with stochastic efficiency of forecast ranging from 69% at Doi Chiang Dao Watershed Research station with correlation coefficient equal to 0.81 to 78% at A. Samoeng station with correlation coefficient equal to 0.82. Moreover, the best performance was obtained for one-month leading time of forecast with stochastic efficiency of forecast ranging from 74% at Doi Chiang Dao Watershed Research station with correlation coefficient equal to 0.81 to 85% at A. Samoeng station with correlation coefficient equal to 0.83.

However, variation in both predictive LAV as input to DNN model and model architecture for each rainfall station reflects characteristics of the black-box model, which cannot be used to describe the physical meaning and mechanism of natural processes. Nevertheless, the DNN model coupling with the input section technique, developed in this study, can be an alternative approach for water resources management and planning. Further study for improvement of accuracy of the long-term forecast as well as the application of a model for water resources planning and drought warning system will be conducted to make the model more useful for sustainable development.

10. Acknowledgements

This research has been supported by the Faculty of Engineering, Thammasat University. Appreciation is also extended to Thai Meteorological department for providing hydrological data used in the study.

11. References

[1] Yu PS, Yang TC, Chen SY, Kuo CM, Tseng HW. Comparison of random forests and support vector machine for real-time radar-derived rainfall forecasting. J Hydrol. 2017;552:92-104.

[2] Abdourahamane ZS, Acar R, Serkan Ş. Wavelet–copula-based mutual information for rainfall forecasting applications. Hydrolog Process. 2019;33(7):1127-42.

[3] Mekanik F, Imteaz MA, Talei A. Seasonal rainfall forecasting by adaptive network-based fuzzy inference system (ANFIS) using large scale climate signals. Clim Dynam. 2016;46(9-10):3097-111.

[4] Acharya R, Pal J, Das D, Chaudhuri S. Long-range forecast of Indian summer monsoon rainfall using an artificial neural network model. Meteorol Appl. 2019;26(3):347-61.

[5] Mishra N, Soni HK, Sharma S, Upadhyay AK. Development and analysis of artificial neural network models for rainfall prediction by using time-series data. Int J Intell Syst Appl. 2018;10(1):16-23.

[6] Khalili N, Khodashenas SR, Davary K, Baygi MM, Karimaldini F. Prediction of rainfall using artificial neural networks for synoptic station of Mashhad: a case study. Arab J Geosci. 2016;9(13):624.

[7] Babel MS, Badgujar GB, Shinde VR. Using the mutual information technique to select explanatory variables in artificial neural networks for rainfall forecasting. Meteorol Appl. 2015;22(3):610-6.

[8] Alotaibi K, Ghumman AR, Haider H, Ghazaw YM, Shafiquzzaman M. Future predictions of rainfall and temperature using GCM and ANN for arid regions: a case study for the Qassim Region, Saudi Arabia. Water. 2018;10(9):1260.

[9] Beheshti Z, Firouzi M, Shamsuddin SM, Zibarzani M, Yusop Z. A new rainfall forecasting model using the CAPSO algorithm and an artificial neural network. Neural Comput Appl. 2016;27(8):2551-65.

[10] Singh P, Borah B. Indian summer monsoon rainfall prediction using artificial neural network. Stoch Environ Res Risk Assess. 2013;27:1585-99.

[11] Hung NQ, Babel MS, Weesakul S, Tripathi NK. An artificial neural network model for rainfall forecasting in Bangkok, Thailand. Hydrol Earth Syst Sci. 2009;13:1413-25.

[12] Sulaiman J, Wahab SH. Heavy rainfall forecasting model using artificial neural network for flood prone area. In: Kim K, Kim H, Baek N, editors. IT Convergence and Security 2017. Singapore: Springer; 2018. p. 68-76.

[13] Nourani V, Uzelaltinbulat S, Sadikoglu F, Behfar N. Artificial intelligence based ensemble modeling for multi-station prediction of precipitation. Atmosphere. 2019;10(2):80.

[14] Kumar D, Singh A, Samui P, Jha RK. Forecasting monthly precipitation using sequential modelling. Hydrolog Sci J. 2019;64(6):690-700.

[15] Luo J, Lu W, Ji Y, Ye D. A comparison of three prediction models for predicting monthly precipitation in Liaoyuan city, China. Water Sci Tech Water Supply. 2016;16(3):845-54.

[16] Devi SR, Arulmozhivarman P, Venkatesh C, Agarwal P. Performance comparison of artificial neural network models for daily rainfall prediction. Int J Autom Comput. 2016;13(5):417-27.

[17] Hamidi O, Poorolajal J, Sadeghifar M, Abbasi H, Maryanaji Z, Faridi HR, et al. A comparative study of support vector machines and artificial neural networks for predicting precipitation in Iran. Theor Appl Climatol. 2015;119(3-4):723-31.

[18] Ramana RV, Krishna B, Kumar SR, Pandey NG. Monthly rainfall prediction using wavelet neural network analysis. Water Resour Manag. 2013;27(10):3697-711.

[19] Mehr AD, Nourani V, Khosrowshahi VK, Ghorbani MA. A hybrid support vector regression–firefly model for monthly rainfall forecasting. Int J Environ Sci Tech. 2019;16(1):335-46.

[20] Yaseen ZM, Ghareb MI, Ebtehaj I, Bonakdari H, Siddique R, Heddam S, et al. Rainfall pattern forecasting using novel hybrid intelligent model based ANFIS-FFA. Water Resour Manag. 2018;32(1):105-22.

[21] Feng Q, Wen X, Li J. Wavelet analysis-support vector machine coupled models for monthly rainfall forecasting in arid regions. Water Resour Manag. 2015;29(4):1049-65.

[22] Weesakul U, Kaewprapha P, Boonyuen K, Mark O. Deep learning neural network: A machine learning approach for monthly rainfall forecast, case study in eastern region of Thailand. Eng Appl Sci Res. 2018;45(3):203-11.

[23] Weesakul U, Singhrattna N, Viwat H. Identification of large-scale atmospheric predictors for rainfall forecasting of Nan River Basin (Thailand). Proceedings of the 5th National Water Resources Engineering Symposium; 2013 Sep 5-6; Chiengrai, Thailand.
[24] Weesakul U, Singhrattna N, Luangdilok N. Identification of large-scale atmospheric predictors for rainfall forecasting of Chi River Basin (Thailand). Proceedings of the 5th National Water Resources Engineering Symposium; 2013 Sep 5-6; Chiengrai, Thailand.
[25] Weesakul U, Singhrattna N, Yodpongpiput P. Statistical relationships between large-scale atmospheric variables and rainfall in Mun River Basin (Thailand). Proceedings of the 5th National Water Resources Engineering Symposium; 2013 Sep 5-6; Chiengrai, Thailand.
[26] Weesakul N, Singhrattna N, Khetped N. Large-scale atmospheric variables influencing on rainfall in Tapee River Basin (Thailand). Proceedings of the 5th National Water Resources Engineering Symposium; 2013 Sep 5-6; Chiengrai, Thailand.
[27] Zhang G, Patuwo BE, Hu MY. Forecasting with artificial neural networks: Int J Forecast. 1998;14(1):35-62.
[28] ASCE Task Committee on Application of Artificial Neural Networks in Hydrology. Artificial neural networks in hydrology. I: Preliminary concepts. J Hydrolog Eng. 2000;5(2):115-23.
[29] Hinton GE, Osindero S, Teh YW. A fast learning algorithm for deep belief nets. Neural Comput. 2006;18(7): 1527-54.
[30] Sheela KG, Deepa SN. Review on methods to fix number of hidden neurons in neural networks. Math Probl Eng. 2013;2013:1-11.
[31] Hunter D, Yu H, Pukish, III MS, Kolbusz J, Wilamowski BM. Selection of proper neural network sizes and architectures—a comparative study. IEEE Trans Industr Inform. 2012;8(2):228-40.
[32] Zhang Z, Ma X, Yang Y. Bounds on the number of hidden neurons in three-layer binary neural networks. Neural networks. 2003;16(7):995-1002.
[33] Rumelhart DE, Hintont GE, Williams RJ. Learning representations by back-propagating errors. Nature. 1986;323(6088):533-6.
[34] May R, Dandy G, Maier H. Review of input variable selection methods for artificial neural networks. In: Suzuki K, editor. Artificial neural networks - methodological advances and biomedical applications. Croatia: IntechOpen; 2011. p. 19-44.
[35] Blum AL, Langley L. Selection of relevant features and examples in machine learning. Artif Intell. 1997;97(1-2):245-71.
[36] Guyon I, Elisseeff A. An introduction to variable and feature selection. J Mach Learn Res. 2003;3:1157-82.
[37] Dariane AB, Azimi Sh. Forecasting streamflow by combination of a genetic input selection algorithm and wavelet transforms using ANFIS models. Hydrolog Sci J. 2016;16(3):585-600.
[38] Abbot J, Marohasy J. Input selection and optimisation for monthly rainfall forecasting in Queensland, Australia, using artificial neural networks. Atmos Res. 2014;138: 166-78.